



LJMU Research Online

Davies, MJ, Leach, AG and Riley, F

An Investigation into Drug Partitioning Behaviour in Simulated Pulmonary Surfactant Monolayers with Associated Molecular Modelling

<http://researchonline.ljmu.ac.uk/id/eprint/7910/>

Article

Citation (please note it is advisable to refer to the publisher's version if you intend to cite from this work)

Davies, MJ, Leach, AG and Riley, F (2018) An Investigation into Drug Partitioning Behaviour in Simulated Pulmonary Surfactant Monolayers with Associated Molecular Modelling. Surface and Interface Analysis. ISSN 1096-9918

LJMU has developed **LJMU Research Online** for users to access the research output of the University more effectively. Copyright © and Moral Rights for the papers on this site are retained by the individual authors and/or other copyright owners. Users may download and/or print one copy of any article(s) in LJMU Research Online to facilitate their private study or for non-commercial research. You may not engage in further distribution of the material or use it for any profit-making activities or any commercial gain.

The version presented here may differ from the published version or from the version of the record. Please see the repository URL above for details on accessing the published version and note that access may require a subscription.

For more information please contact researchonline@ljmu.ac.uk

<http://researchonline.ljmu.ac.uk/>

1 **An Investigation into Drug Partitioning Behaviour in Simulated Pulmonary Surfactant Monolayers**
2 **with Associated Molecular Modelling**

3
4 Michael J. Davies^{a,*}, Andrew G. Leach^a & Fatima Riley^a

5 ^aThe School of Pharmacy and Biomolecular Sciences, Liverpool John Moores University, Liverpool, L3 3AF, UK.
6

7 **Abstract**

8 Drug delivery to the body via the inhaled route is dependent upon patient status, device use and respirable
9 formulation characteristics. Further to inhalation, drug-containing particles interact and dissolve within
10 pulmonary fluid leading to the desired pharmacological response. Pulmonary surfactant stabilises the alveolar
11 air-liquid interface and permits optimal respiratory mechanics. This material represents the initial contacting
12 surface for all inhaled matter. On dissolution, the fate of a drug substance can include receptor activation,
13 membrane partitioning and cellular penetration. Here, we consider the partitioning behaviour of salbutamol
14 when located in proximity to a simulated pulmonary surfactant monolayer at pH 7. The administration of
15 salbutamol to the underside of the surfactant film resulted in an expanded character for the two-dimensional
16 ensemble and a decrease in the compressibility term. The rate of drug partitioning was greater when the
17 monolayer was in the expanded state (i.e. inhalation end-point), which was ascribed to more accessible areas
18 for molecular insertion. Quantum mechanics protocols, executed via Gaussian 09, indicated that constructive
19 interactions between salbutamol and integral components of the model surfactant film took the form of
20 electrostatic and hydrophobic associations. The favourable interactions are thought to promote drug insertion
21 into the monolayer structure leading to the observed expanded character. The data presented herein confirm
22 that drug partitioning into pulmonary surfactant monolayers is a likely prospect further to the inhalation of
23 respirable formulations. As such, this process holds potential to reduce drug-receptor activation and / or
24 increase the residence time of drug within the pulmonary space.

25
26
27
28
29 *Key words*

30
31 Pulmonary surfactant, Langmuir monolayers, inhaled drug delivery, salbutamol sulphate, molecular
32 modelling, Gaussian 09.

33
34 *Corresponding Author Details:*

35
36 * To whom correspondence should be addressed:

37 Tel. (+44) 0151 231 2024

38 Email: m.davies1@ljmu.ac.uk

39 Fax. (+44) 0151 231 2170

40 1. Introduction

41

42 The respiratory system can be principally divided into two regions, namely the upper and lower
43 airways. The former marks the point of entry for atmospheric gases, respirable formulations and
44 environmental toxins, whilst the latter is the primary site for gaseous exchange and holds the potential
45 to be exploited for drug (i.e. insulin and analgesic) delivery to the systemic circulation [1]. Drug
46 deposition within the respiratory tract as a whole is dependent on a number of factors including for
47 instance inhaler technique, patient co-morbidities, device structure and function plus formulation
48 characteristics (i.e. drug particle size, shape, density, surface energetics and external chemistries) [2].
49 Typically, the dose of medicine physically delivered to the lung on device activation is within the region
50 of 20% of that emitted at source [3]. At the early stage of the drug delivery process, the aerodynamic
51 particle size of the solid material heavily influences deposition patterns. For example, those particles
52 of diameter 5 μ m or less hold a good chance of deep lung deposition with drug particles of less than
53 3 μ m diameter able to reach the alveolar space [4]. Following delivery to the deep lung and related
54 interaction with the respective internal surfaces, individual drug-containing particles and solubilised
55 drug molecules must overcome a number of barriers (e.g. pulmonary surfactant and the lung epithelial
56 layer) and processes (e.g. mucociliary clearance and partitioning) prior to local or systemic activity [5].
57 A robust understanding of the fate of inhaled therapies, and of particular relevance to the work
58 presented herein drug partitioning within pulmonary surfactant monolayers, can inform the drug
59 design process and consequently lead to improved respirable formulations.

60 Pulmonary surfactant is central to effective respiratory mechanics. This endogenous material bathes
61 the alveolar air-liquid interface and preserves airway patency by reducing the work of breathing [6].
62 In addition, the substance protects the lung from invading microorganisms, environmental toxins and
63 particles inhaled from the atmosphere by promoting the process of mucociliary clearance [7]. The
64 lipid element of pulmonary surfactant accounts for 90% of the blend and consists of several species
65 such as phosphatidylcholines (PC), unsaturated phosphatidylglycerols (POPG) along with cholesterol,
66 fatty acids and triglycerides plus palmitic acid (PA). Dipalmitoylphosphatidylcholine (DPPC) is the most
67 abundant phospholipid within pulmonary surfactant, ranging from between 40% - 80% by weight [8].
68 This particular species packs tightly at the interface and reduces surface tension to near zero values
69 from the maximum surface pressure of 70mN/m [8]. Surfactant specific proteins (SP) account for the
70 remaining 10% of the mixture and include SP-A, SP-B, SP-C and SP-D; all differ in molecular weight,
71 size and function [7].

72

73 Detailed discussion regarding the chemistries of key components of model pulmonary surfactant (i.e.
74 DPPC, POPG and PA) [9] has been provided elsewhere [10], hence consideration will be limited here.
75 In brief, the DPPC molecule exists as a zwitterion at physiological pH [11] and includes two saturated
76 acyl chains which assemble through hydrophobic interactions into gel-like condensed phases [12]. The
77 quaternary ammonium group that holds a permanent charge can act as a non-classical hydrogen bond
78 donor. In addition, a hydrogen bond acceptor is present within the molecule as a result of the
79 negatively charged phosphate group; unlike the positive charge, the negative charge is pH dependant.
80 Post compression, DPPC is unable to reform the monolayer rapidly as high surface pressures promote
81 the solid state. Therefore, additional lipid species are required to improve and facilitate material
82 respread during inspiratory phases [8] Indeed, this particular point has been highlighted by
83 Veldhuizen and co-workers who demonstrated that DPPC:PG mixtures increased adsorption activity
84 compared to single component mixtures alone [13]. In relation to this, it is widely acknowledged that
85 surfactant specific proteins are central in promoting material respread, adsorption and stabilisation
86 of the surface film during the breathing process [14]. The 1-palmitoyl-2-oleyl-phosphatidylglycerol
87 (POPG) molecule is an unsaturated anionic phospholipid that increases the fluidity of a two-
88 dimensional surfactant film and enhances adsorption at the air-liquid interface post compression. This
89 fluidising agent has a similar chemical structure to DPPC, however the quaternary ammonium group
90 is replaced with two hydroxyl groups and bears one negative charge per molecule in the form of a
91 phosphate group [10]. Palmitic acid is composed of a 16-carbon acyl chain that makes up the fatty
92 acid component of some phospholipids and improves the surface properties of the surfactant,
93 especially DPPC. This particular molecule is a long chain saturated fatty acid with a terminal carboxylic
94 acid group. The species enhances the rigidity of a pulmonary surfactant monolayer at low surface
95 tensions and facilitates respreading; thus supporting its inclusion within model pulmonary surfactant
96 formulations considered in this work [9].

97 The application of Langmuir monolayer technology to study pulmonary surfactant relies upon the
98 careful arrangement of amphiphilic molecules across the surface of an aqueous subphase such that
99 the hydrocarbon chain components direct themselves towards the gaseous phase (i.e. air) and related
100 polar functionalities penetrate into the liquid phase (i.e. ultrapure water). Once established, scope
101 exists to apply lateral forces to the surfactant film either in isolation (i.e. Langmuir isotherm) or in
102 rapid succession (i.e. Langmuir isocycle) to probe structure-function activity. Interestingly,
103 opportunity also presents to hold the surfactant molecules in a fixed position at a particular target
104 pressure and observe the impact of molecular interactions on material dynamics over time.

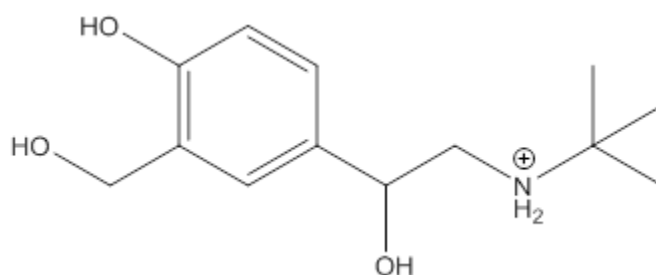
105

106 Such Langmuir surface pressure – time plots, leading to penetration pressure – time data series, can
107 be readily applied to better understand the interaction between drug molecules dissolved within the
108 supporting subphase and the two-dimensional ensemble under investigation (i.e. to assist in the
109 determination of drug partitioning behaviour within a simulated pulmonary space).

110 Drug partitioning is the distribution of therapeutic molecules between two immiscible phases, where
111 an aqueous solution is usually present [15]. The ability to achieve certain concentrations in different
112 phases underpins diffusion of molecules which is fundamental in the process of drug delivery to the
113 body and in particular drug absorption leading to a therapeutic response. Clearly, the degree to which
114 drug partitioning occurs is dependent on the properties of the surrounding phases and respective
115 chemical components. Most drug molecules may be ionised in solution resulting in either anionic,
116 cationic, zwitterionic or neutral forms; the extent of which depends on the acidity or basicity of the
117 drug and relative pH of the solution. Naturally, the ionisation state of a therapeutic molecule can
118 significantly impinge upon the partition index (i.e. in terms of lipid solubility within a surfactant film
119 moving from solvent water). Additional factors that may influence drug partitioning include the size,
120 shape and concentration of the drug molecule itself [16]. To date, relatively few studies have
121 considered drug (in the present case salbutamol sulphate) penetration into simulated pulmonary
122 surfactant monolayers and rationalised the resultant biological outcomes. This fact may be ascribed
123 to the inherent complexity of the systems involved [15]. However, applied research in this field is
124 possible with evidence emerging that drug partitioning within such a space can occur via unassisted
125 thermodynamic mechanisms. For example, in 1998 Krill and colleagues highlighted that initial
126 penetration and subsequent partitioning of a drug into a two-dimensional lipid film can be either
127 enthalpically or entropically driven, or indeed both [17].

128 Salbutamol sulphate is widely prescribed within the United Kingdom for the management of asthma
129 and chronic obstructive pulmonary disease (COPD) [18]. This therapeutic agent is a short acting β_2 -
130 adrenergic receptor agonist that initiates relaxation of bronchial smooth muscle post administration
131 [3]. The onset of action following inhalation is typically 5 minutes and the therapeutic effect normally
132 remains for between 3 and 5 hours [18]. The recommended daily inhaled dose of salbutamol sulphate
133 is usually 100mcg – 200mcg up to four times a day, as required [18]. The high selectivity for β_2 -
134 adrenoceptors may be ascribed to the N-t-butyl group within the molecule, as detailed in Figure 1
135 [19].

136



137

138 **Figure 1.** *The molecular structure of salbutamol.*

139 Salbutamol presents as a racemic mixture, where the R-isomer is pharmacologically active and holds
140 high affinity for β_2 -adrenoceptors as compared to the S-isomer [11]. The chemical stability of
141 salbutamol sulphate can be affected by pH, elevated temperatures and buffer solutions. As the
142 ionisation state of salbutamol varies with pH, the molecule can exist in either a zwitterionic or cationic
143 form having the two pKa values of 9.3 (i.e. amino) or 10.3 (i.e. phenolic), respectively [11, 20].
144 Protonation of the nitrogen atom within the salbutamol structure can promote ionic bond formation
145 with negatively charged functionalities of neighbouring molecules (i.e. phosphate groupings available
146 within nearby DPPC and POPG surfactant species). Furthermore, hydrogen bonds may also form with
147 the phenolic groups in salbutamol.

148 Surface electrostatic potentials relating to therapeutic drug molecules of interest (i.e. salbutamol) and
149 the polar regions of amphiphilic molecules located at the alveolar air-liquid interface (i.e. DPPC, POPG
150 and PA) may be determined via the execution of quantum mechanics protocols. Indeed, such
151 calculations have been successfully applied in recent studies conducted by Clark and co-workers
152 during 2007 [21] plus Davies and colleagues in 2017 [10]. The understanding gained can further our
153 appreciation of how interacting moieties arrange themselves when in close proximity to each other
154 and how such arrangement can dictate drug impact on system function and activity within the body.
155 Density functional theory can provide electrostatics of sufficient accuracy to explain drug-surface
156 interactions [22]. Accordingly, this approach will be applied to rationalise information obtained from
157 Langmuir monolayer studies such that deviations in isotherms / isocycles from the baseline can be
158 mechanistically explained.

159 This study aims to investigate the partitioning behaviour of our model therapeutic agent salbutamol
160 sulphate when injected to the underside of simulated pulmonary surfactant monolayers at pH 7.
161 Associated molecular modelling will be conducted to rationalise key interactions at the molecular
162 level. The results obtained will be related to the fate of drug entities on delivery to the respiratory
163 tract.

164

2. Materials and Methods

2.1 Materials

Salbutamol sulphate was purchased from BUFA Chemicals, Germany (Charge: 13K26-B07-296570. Art. Nr. 13010). The surfactants DPPC (BN: 160PC-319) and POPG (BN: 160-181PG-137) were obtained from Avanti Polar Lipids, USA, whilst PA was acquired from Sigma-Aldrich, UK (BN: 087K1877). The materials were of analytical grade and used as supplied. Chloroform (CHCl_3) was also of analytical grade ($\geq 99.9\%$) and purchased from Fischer Scientific, UK (BN: 1693191). This solution was employed to dissolve the surface active material to form the Langmuir trough spreading solution and for all cleaning procedures. Ultrapure water (Purite, UK), of resistivity $18. \text{M}\Omega\text{cm}$, was used both during cleaning procedures and as the aqueous subphase during all Langmuir monolayer work.

2.2 Method

2.2.1 Langmuir Monolayers

Simulated pulmonary surfactant monolayers were generated using a Langmuir trough (Model 102M, Nima Technology, UK). Surfactant-free Kimtech tissues (Kimtech Science, Kimberley-Clark Professional, 75512, UK) were soaked in chloroform and used to clean all the glassware and contacting surfaces. Trough cleanliness was confirmed by application of surface pressure test runs, where a value of 0.4mN/m (or less) at full barrier compression confirmed suitability. A chloroform-based spreading solution composed of DPPC, POPG and PA in the ratio 69:20:11 was produced at a concentration of 1mg/ml [9]. Subsequently, a volume of $15 \mu\text{l}$ of the spreading solution was applied to the surface of the aqueous subphase by drop-wise addition and a period of 10 minutes allowed to enable monolayer settling. The Langmuir trough barriers were set to move to the centre of the trough at a rate of $25 \text{cm}^2/\text{min}$ in the case of isotherm plots. With regard to Langmuir isocycle data, the barrier system was programmed to operate at $100 \text{cm}^2/\text{min}$. Surface pressure vs percentage trough area readings under ambient conditions (i.e. $20^\circ\text{C} \pm 1^\circ\text{C}$) were collected using a Wilhelmy plate at the centre of the compartment.

199 To examine the rate of drug partitioning with respect to time, the target pressures of 10mN/m (i.e.
200 inhalation end-point) and 50mN/m (i.e. exhalation end-point) were established and left to stand for
201 one hour. Here, the first 5 minutes were used to condition the monolayer and salbutamol sulphate
202 was then injected underneath the monolayer at the 5th minute, as detailed in the following section.
203 Data was then acquired after the 10th minute to allow the monolayer to settle upon addition of the
204 drug. All data were acquired in triplicate and the standard error of the mean calculated accordingly.
205 The analysis of covariance was elucidated in order to test for significance within the time-based data
206 sets.

207 2.2.2 Salbutamol Sulphate Administration to Simulated Pulmonary Surfactant Monolayers

208

209 Initially, 2mg of salbutamol sulphate was accurately weighed and then dissolved in 1ml of ultrapure
210 water to obtain a stock solution of concentration 2mg/ml. This drug-containing solution was
211 subsequently diluted 5 times by removing 100 μ l of solution and adding this to 900 μ l of ultrapure
212 water. On completion of this process, the concentration of the final salbutamol sulphate solution was
213 0.02mcg/ml. Further to a period of 10 minutes for mixed surfactant monolayer spreading, the pre-
214 prepared salbutamol-containing solution was delivered to the underside of the two-dimensional film
215 (i.e. to reflect drug availability post particle dissolution). Here, a volume of 500 μ l of the diluted
216 salbutamol solution was added to either side of the compartment underneath the trough barriers. On
217 delivery a period of 10 minutes allowed the drug to distribute evenly within the supporting subphase
218 and interact within the simulated pulmonary surfactant monolayer. Langmuir isotherms, isocycles
219 and surface pressure – time data were then generated for each system under investigation. Each
220 investigation was repeated in triplicate with the standard error of the mean in turn calculated.

221 To investigate dose response effects, individual Langmuir isotherms and isocycles were obtained with
222 concentrations of 0.01mcg/ml, 0.02mcg/ml and 0.04mcg/ml of salbutamol; where a total of 1mg, 2mg
223 and 4mg were diluted 5 times as previously described. In this case, the dose conversion from 200mcg
224 (i.e. two standard doses) to 0.02mcg/ml was calculated as a factor of the surface area of the Langmuir
225 trough. Here, the Langmuir trough area was 70cm², whilst the surface area of the lung is recognised
226 to be 70m² [23].

227

228

229

230

231 2.2.3 Langmuir Monolayer Analysis

232

233 2.2.3.1 Compressibility

234

235 The compressibility term relates to the ability of a surfactant film to reduce the surface tension term
236 with minimal transformation to surface area [24]. An ideal lung surfactant should have a low
237 compressibility value as this indicates the rigidity of the monolayer which represents *in vivo*
238 conditions [25]. To calculate the compressibility term, Equation 1 was employed.

239

240
$$\text{Compressibility} = \frac{1}{A} \times \frac{1}{m}$$

241

242 **Equation 1.** Calculation of the compressibility of the monolayer.

243

244 Where A represents the relative surface area and m the slope of the isotherm. Here, 'm' was calculated
245 using 'm = $\frac{y_2 - y_1}{x_2 - x_1}$ ', between 50% and 80% of the Langmuir trough area.

246

247 2.2.3.2 Statistical Analysis

248

249 With respect to Langmuir surface pressure - time data, statistical analysis involved application of
250 analysis of covariance using Minitab v17 [26]. This software was utilised to compare the mean of each
251 data point with time and pressure. Here, a 'p' value of <0.05 was used to demonstrate significance.

252

253

254

255

256

257

258

259

260

261

262

263

264

265

266 2.2.4 Molecular Modelling

267
268

269 In order to rationalise drug partitioning behaviour in proximity to simulated pulmonary surfactant
270 monolayers, system components were studied at the RHF/6-31G* level via Gaussian09 [27, 28, 29,
271 30]. Conformations of the key elements for molecular recognition at the underside of the surfactant
272 monolayer (i.e. excluding the more external hydrocarbon chain groupings) were generated using
273 omega [31]. Following geometry optimisation, the electron density was visualised in Gaussview [32].
274 Here, the electrostatic potential is projected onto a surface of constant electron density using default
275 values. Representations of the projected electrostatic potential were generated from two opposing
276 sides. The resultant output was the generation of a number of images that reflect all of the entities
277 that could potentially interact at the test interface.

278

279 **3 Results and Discussion**

280
281

282 During this work we have applied a mixed surfactant monolayer composed of primary lipid species of
283 the lung (i.e. DPPC, POPG and PA) to represent the alveolar air-liquid interface within the laboratory
284 setting. Throughout, the dynamic interplay between constituents of the thin lipid films and drug
285 molecules was considered. The overarching intention was to determine the mechanism(s) of
286 salbutamol interaction with simulated pulmonary surfactant monolayers and hence better
287 understand drug partitioning behaviour further to delivery to the respiratory tract.

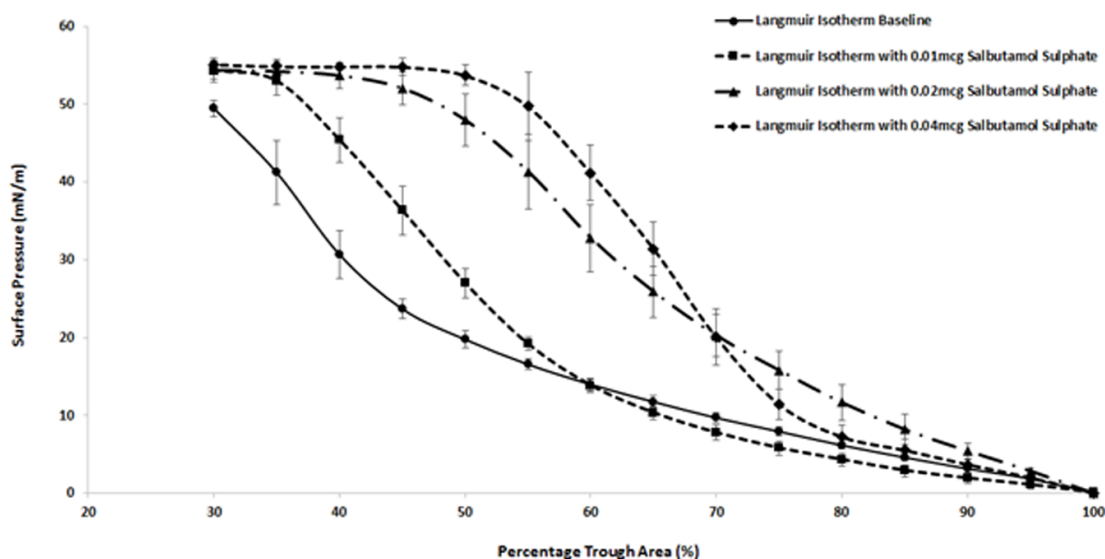
288

289 *3.1 Langmuir Isotherms*

290

291 Langmuir pressure-area (π -A) isotherms of the mixed monolayer system following exposure to
292 increased concentrations of salbutamol sulphate are presented in Figure 2.

293



294

295 **Figure 2.** Langmuir π -A isotherms for the mixed surfactant system supported on an ultrapure water subphase
 296 with increased concentrations of salbutamol sulphate at pH 7. In each case, a total of 3 repeats were acquired
 297 to enable the presentation of average values with error bars representing one standard error in the mean. All
 298 experiments were conducted at a temperature of $20^{\circ}\text{C} \pm 1^{\circ}\text{C}$.

299 On inspection of the data presented in Figure 2, it is evident that compression of the mixed monolayer
 300 system led to an increase in the surface pressure term throughout. In all cases smooth traces are
 301 apparent and are in line with previously acquired data [10]. Clear gradient changes within each curve
 302 reflect phase transitions within the two-dimensional ensemble [33]. Baseline data confirmed that the
 303 mixed surfactant film attained a maximum surface pressure of 49mN/m. However, this value
 304 increased upon salbutamol sulphate addition to the supporting aqueous subphase; the maximum
 305 surface pressure was above 54mN/m, for all concentrations of salbutamol sulphate that were studied.
 306 The apparent increase in the surface pressure term was attributed to the drug contribution at the air-
 307 liquid interface within the test zone.

308 Administration of salbutamol sulphate to the mixed surfactant monolayer caused a change to the
 309 Langmuir isotherm shape when compared to the baseline. Here, expansion of the two-dimensional
 310 ensemble is consistently demonstrated, being concentration dependent. The delivery of 0.01mcg
 311 salbutamol sulphate to the test zone resulted in monolayer expansion, with a maximum surface
 312 pressure of 54.3mN/m recorded; a comparable value to the 0.02mcg/ml addition. Whilst the delivery
 313 of 0.04mcg/ml salbutamol sulphate to the supporting aqueous media resulted in an increase in the
 314 surface pressure term to 55.1mN/m. This equates to a 1.5% increase in maximum surface pressure
 315 from the addition of 0.02 mcg of salbutamol. The Langmuir isotherm data also indicate that as the
 316 concentration of salbutamol sulphate increases, the curve plateau point is realised at an earlier stage.

317 For doses 0.01mcg, 0.02mcg and 0.04mcg the isotherm starts to plateau at trough areas of 35%, 40%
318 and 50% which confirms a greater solid phase contribution to monolayer dynamics.

319 On consideration of the compressibility term, a decrease in the descriptor was evident on increasing
320 salbutamol sulphate concentration as outlined in Table 1 (e.g. the addition of 0.04 mcg/ml caused an
321 approximate 70% reduction from the baseline value). The clear reduction in this parameter confirms
322 that as the number of drug molecules increase, the two-dimensional film becomes more rigid and less
323 compressible.

324

Surface Area (%)	Baseline (Monolayer)	Salbutamol (0.01mcg)	Salbutamol (0.02mcg)	Salbutamol (0.04mcg)
80	0.0268	0.0163	0.0101	0.0082
70	0.0306	0.0187	0.0115	0.0093
60	0.0358	0.0218	0.0135	0.0109
50	0.0429	0.0261	0.0162	0.0130

329

330 **Table 1.** Compressibility values (mN/m) of the Langmuir surface pressure isotherms.

331 Drug insertion into a surfactant film influences lipid packing and hence system dynamics. Here, the
332 addition of salbutamol sulphate to the underside of the pulmonary surfactant monolayer, plus related
333 molecular interaction, led to increased rigidity and a more rapid increase in the surface pressure
334 term. The net effect is the presentation of the condensed / solid phases at an earlier point in time.
335 This is due to an increase in the number of molecules over a constant surface area. The process by
336 which the drug molecule can partition into the monolayer and diffuse out can also be explained by
337 the inhomogeneous solubility-diffusion mechanism [34]. This involves a three-step process by which
338 the molecule partitions in, diffuses within the structure and to an extent partitions out, which depends
339 on thermodynamic driving forces of the complete system under investigation.

340 On delivery of the drug-containing solutions (e.g. 0.02mcg/ml) to the supporting aqueous subphase,
341 a further dilution took place in the average volume of 41ml (n=3) of ultrapure water held within the
342 Langmuir trough. Upon addition of 1ml of the 0.02mcg, this would equate to a final concentration of
343 4.76×10^{-4} mcg/ml of salbutamol sulphate in the subphase. Furthermore, an addition of 0.01mcg and
344 0.04mcg would further dilute the drug to a concentration to 2.38×10^{-4} mcg/ml and 9.52×10^{-4} mcg/ml,
345 respectively.

346 This indicates that with highly diluted drug concentrations scope exists for partitioning into the
347 monolayer, which is shown by translocation of the curves to the right. Indeed, this effect was reported
348 by Jablonowska and Bilwicz during 2007 where the group demonstrated that ibuprofen diluted to
349 concentrations of 2×10^{-5} – 2×10^{-4} M caused changes in the compressibility of a surfactant monolayer
350 with partitioning still occurring at low concentrations [35].

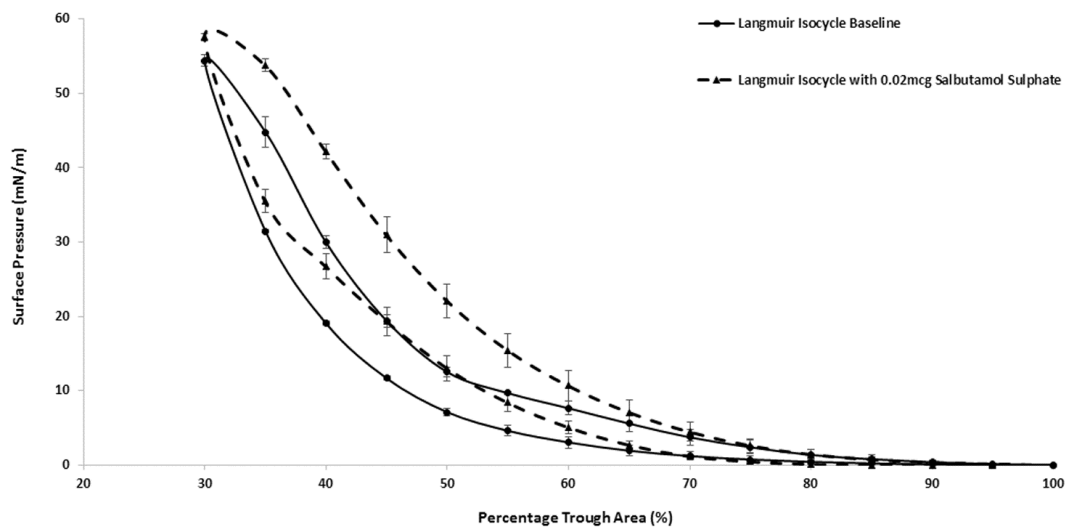
351

352 3.2 Langmuir Isocycles

353

354

355 Average Langmuir compression-expansion cycles of the simulated pulmonary surfactant monolayer
356 system at pH 7 pre- and post-salbutamol sulphate addition are presented in Figure 3. The data
357 presented are averages of three replicates of the same.



358

359 **Figure 3.** Average Langmuir π -A isocycles for the mixed surfactant system supported on an ultrapure water
360 subphase with a salbutamol sulphate concentration of 4.76×10^{-4} mcg/ml at pH 7. In each case, 3 repeats were
361 acquired and points are the mean with error bars of one standard error in the mean. The experiments were
362 conducted at a temperature of $20^\circ\text{C} \pm 1^\circ\text{C}$.

363

364 During Langmuir pressure – area isocycle generation, initial pre-conditioning inward and outward
365 sweeps were executed (n=4). The purpose of this procedure was to prepare the conformation of the
366 mixed monolayer system to best represent that noted within the (deep) human lung. Clearly, this
367 approach differs from a single compression isotherm in that the constituent molecules are arranged
368 more favourably and typical of the physiologically relevant scenario.

369 This pre-conditioning stage and removal of associated early phase traces (n=4) results in the
370 elimination of the solid phase plateau noted in single Langmuir pressure – area isotherms (i.e. those
371 shown in Figure 2).

372 On monolayer cycling, the maximum surface pressure for the mixed surfactant system was 54.4mN/m.
373 However, on addition of salbutamol sulphate this value increased to 57.6mN/m; equating to a 6%
374 increase in the term. Once again, the data indicate that further to the addition of salbutamol sulphate
375 to the supporting aqueous media the monolayer becomes expanded in nature (i.e. the Langmuir π -A
376 isocycles translocate to the right). In a similar fashion to that outlined above, the compressibility term
377 also decreased following salbutamol sulphate administration. Here, the baseline value of
378 0.0288mN/m decreased to 0.0203mN/m, representing a 30% reduction in the parameter indicative of
379 reduced flexibility, compressibility and increased rigidity of the monolayer.

380 On completion of the Langmuir isocycle experiments, deviation in the gradient of the trace confirmed
381 amphiphilic molecule phase transitions (i.e. movement from the gaseous phase through to the
382 expanded and condensed phases and ultimately the solid phase). On moving from the gaseous phase
383 to the solid phase, there is a related increase in molecular order. As such, at low surface pressures
384 the monolayer exhibits a certain level of disorder with some spacing between constituent surface
385 active molecules. At the higher surface pressure, the monolayer is decidedly ordered and a tighter
386 molecular packing of DPPC, POPG and PA has occurred resulting in a solid phase transition [36]. Thus,
387 the very state of the surfactant film will govern the propensity of the dissolved drug molecules to
388 partition into the ensemble.

389 The injection of salbutamol sulphate (0.02mcg/ml) into the supporting aqueous subphase caused the
390 gradient of the Langmuir isocycle to become steeper. The data indicate that the phase transitions
391 occur at an earlier point in time, as compared to the baseline. The result can be attributed to an
392 increase in the number of molecules across the two-dimensional plane (i.e. the insertion of drug
393 molecules into the surfactant monolayer). It is the very presence of drug molecules within the system
394 that leads to a more rapid phase transformation and resultant tighter packing at an earlier stage. Such
395 packing causes the presentation of the solid phase sooner than compared to the baseline.

396

397

398

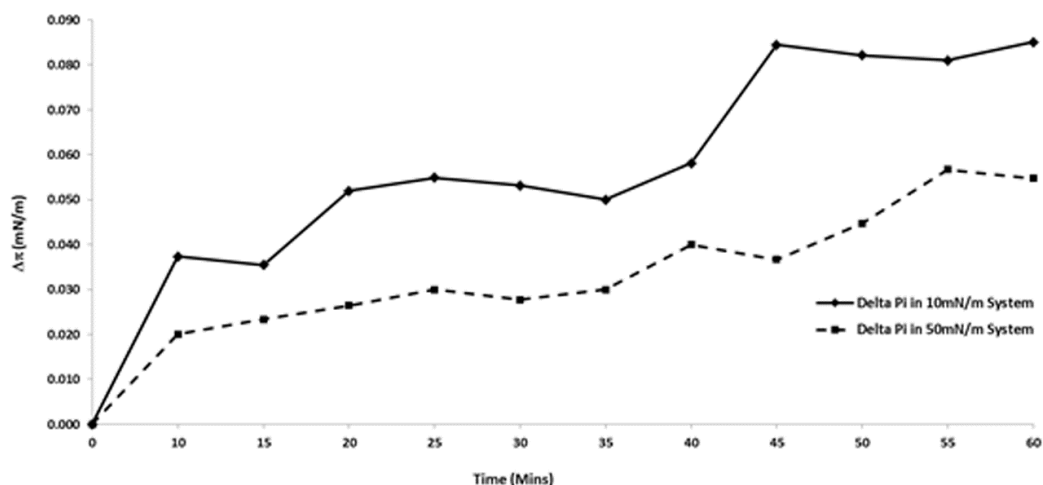
399 Monolayer collapse occurs where lipid components become unstable after maximum surface pressure
400 has been achieved [37]; naturally this situation should be avoided within the laboratory setting. In
401 terms of the Langmuir isotherm baseline data, the simulated pulmonary surfactant monolayer
402 collapsed at the maximum surface pressure of 49.5mN/m. However, typical collapse pressure for a
403 simulated pulmonary surfactant monolayer (i.e. Curosurf® [38]) would be approximately 70mN/m.
404 This parameter is influenced by factors such as the operating temperature and the lipid composition.
405 Thus, we suggest that the lower maximum surface pressure present herein was a combined function
406 of the operating temperature (i.e. 21°C), monolayer composition (i.e. only DPPC, POPG and PA), plus
407 monolayer pre-conditioning stages that involved four repeated compression – expansion events.

408 It is anticipated that to some extent drug partitioning within a surfactant film is reversible as re-
409 spreading occurs on barrier expansion (i.e. representative of inhalation) [37]; particularly at the higher
410 percentage trough areas. Excess lipid material is removed from the subphase into the surface
411 associated reservoir during compression at exhalation. The material is usually composed of
412 unsaturated lipid components where this phenomenon illustrates the molecules are being ‘squeezed
413 out’ from the monolayer. As a result, saturated lipid components at the interface obtain low surface
414 tensions *in vivo*.

415 3.3 Langmuir Surface Pressure – Time Analysis

416

417 During this work, consideration was given to how the physical state of a simulated pulmonary
418 surfactant monolayer (i.e. expanded or compressed) can influence drug partitioning behaviour. To
419 this end, Langmuir surface pressure – time plots were generated. The penetration pressure ($\Delta\pi$) [17,
420 39] data for both the expanded and compressed systems are presented in Figure 4.



421

422 **Figure 4.** Average Langmuir penetration pressure – time plots for the systems under consideration. Each data
 423 point arises from three repeats of the same experiment. Standard error of the mean bars have been included
 424 within the plot, however visibility is limited due to low variability in the data sets. The surface pressure term has
 425 an impact on the partitioning behaviour of salbutamol, with the lower surface pressure offering greater scope
 426 for drug insertion into the two-dimensional film. All data are acquired at pH 7 and a temperature of $20^{\circ}\text{C} \pm 1^{\circ}\text{C}$.

427

428 The addition of salbutamol sulphate (0.02mcg) to the underside of the simulated pulmonary
 429 surfactant monolayer caused an increase in the surface pressure term in both cases with respect to
 430 time. Upon inspection of the data presented in Figure 4, it is evident that the change in surface
 431 pressure ($\Delta\pi$) is greater in the case of the more expanded system (i.e. 10mN/m) and this directly aligns
 432 with the relaxed physical arrangement of the surfactant molecules. Thus, there is a greater propensity
 433 for drug molecules to partition into the two-dimensional surfactant film at the lower surface pressure
 434 (i.e. inhalation end-point). We emphasise that at the target pressure of 50mN/m, the rate of drug
 435 partitioning was slower albeit still taking place (i.e. $P=0.0014$: Langmuir surface pressure – time data,
 436 not shown). Whilst there would be tight molecular order at this pressure, absolute compression does
 437 not occur and consequently there is still the opportunity for salbutamol to interact constructively with
 438 and partition into the monolayer.

439

440

441

442 The data confirm that the physical state of the monolayer can have a significant bearing on the
443 partitioning behaviour of solubilised drug molecules within the underlying vicinity. Typically, the polar
444 head groups of DPPC, POPG and PA are situated deep within the supporting aqueous media at low
445 surface pressures [40, 41]. Thus, a solubilised drug molecule (i.e. arising post drug particle dissolution)
446 can readily interact with the components of the surfactant monolayer and subsequently associate
447 with or penetrate into the two-dimensional structure. It is to be expected that the extent of drug
448 partitioning is likely to be greater at a lower surface pressure (i.e. the point of inhalation) due to the
449 increased likelihood of accessible regions [42, 43] for molecular insertion.

450 Indeed, when we consider the two-dimensional arrangement of the components of a model lung
451 surfactant (i.e. DPPC, POPG and PA) throughout the course of compression and expansion, there is
452 high level of certainty that 'accessible regions' will present to in turn promote drug partitioning. At
453 this juncture, it is appropriate to refer to the work conducted by Bringezu and colleagues in 2003 who
454 probed the impact of environmental tobacco smoke on the primary lipid species of lung surfactant
455 [9]. During the work, the group applied fluorescence microscopy to observe the changes in monolayer
456 structure as lateral compression was applied across the plane. With regard to their pristine system
457 (i.e. identical to that applied during this work), low surface pressures were linked to the presentation
458 of condensed or tightly packed DPPC / PA regions within expanded or more relaxed DPPC / POPG areas
459 consistently visible throughout the surfactant film as a whole. The fluorescent dye applied during the
460 work preferentially distributed itself into the disordered DPPC / POPG regions. As the surface pressure
461 was ramped towards the collapse point, the number of solid phase domains increased. Thus, at the
462 higher surface pressures the monolayer structure became much more ordered. The data presented
463 within the piece confirmed that a surfactant monolayer composed of primary lipid species exhibits
464 non-uniform packing throughout, a feature to be anticipated at the alveolar air-liquid interface within
465 the body.

466 The apparent lack of homogeneity across a lung surfactant film does lend strong support to the
467 concept of 'accessible areas' to promote drug partitioning, as detailed by Vilallonga and Phillips in
468 1978 [39]. This work considered how the anthracycline glycoside antibiotic doxorubicin associated
469 with phospholipid monolayers located at the air-liquid interface. On application of the accessible area
470 calculation (i.e. $a = A - NA_m$) it was established that the condensed monolayer had an average 7%
471 region of access for dissolved drug molecules, as compared to the less condensed monolayer of 33%
472 availability for the same.

473

474 The net effect was a greater increase in the surface pressure term for the more relaxed monolayer
475 system (i.e. there was more area accessible for drug partitioning and as such more drug molecules
476 were able to penetrate into the structure and increase the surface pressure). The group also
477 demonstrated an increase in the surface pressure term in all cases following the injection of drug
478 substance beneath the monolayer structure. The result was ascribed to the 'osmotic approach'
479 leading to an increase in the number of molecular entities at the interface.

480 A similar principle was applied by Krill and co-workers in 1998 who considered the partitioning
481 behaviour of various β -antagonists (e.g. propranolol, oxprenolol, metoprolol and nadolol) when
482 placed in an aqueous environment beneath Langmuir monolayers composed of
483 dimyristoylphosphatidylcholine [17]. Within the study, clear reference was made to the fact that all
484 molecules demonstrated surface activity, irrespective of solution concentration. Importantly,
485 movement into condensed phases of the monolayer structure was noted, which links with the findings
486 presented herein (i.e. a notable change in the presented penetration pressure at the higher value of
487 50mN/m). Thus, throughout tidal breathing one would expect therapeutic entities to associate with
488 and partition into lung surfactant at the alveolar air-liquid interface, irrespective of the surface
489 pressure placed on the endogenous material at any one time. The propensity of this process heavily
490 depends upon the chemical properties of the administered molecule(s). For instance, Krill and
491 colleagues demonstrated that propranolol exhibited the greatest degree of monolayer penetration
492 followed by metoprolol, oxprenolol and finally nadolol. Thermodynamic aspects are central to drug
493 insertion into a surfactant film. For example, Krill noted that propranolol partitioning into the
494 monolayer structure was enthalpically and entropically driven, and this contrasted sternly with
495 nadolol which was mainly enthalpically driven whilst being strongly entropically hindered. It would
496 appear that two key aspects dominate the interaction as a whole; namely, modification to the
497 monolayer structure across the plane plus the physical movement of drug molecules into the lipid
498 layer.

499 Variation in the monomolecular structure results further to drug partitioning with either the drug
500 causing expanded regions to become more condensed in nature via insertion within accessible areas
501 or direct interaction between drug molecule and surfactant components, as modelled herein. Such
502 modification to the surfactant film in the (deep) lung can influence structure-function activity [10],
503 however in general terms the surfactant film appears robust and resilient to external stressors (i.e.
504 drug substances and environmental toxins [43]) and this allows it to fulfil its crucial biological function.

505

506

507 *3.4 Molecular Modelling*

508

509 *3.4.1 Salbutamol Interaction with Surfactant Film Components*

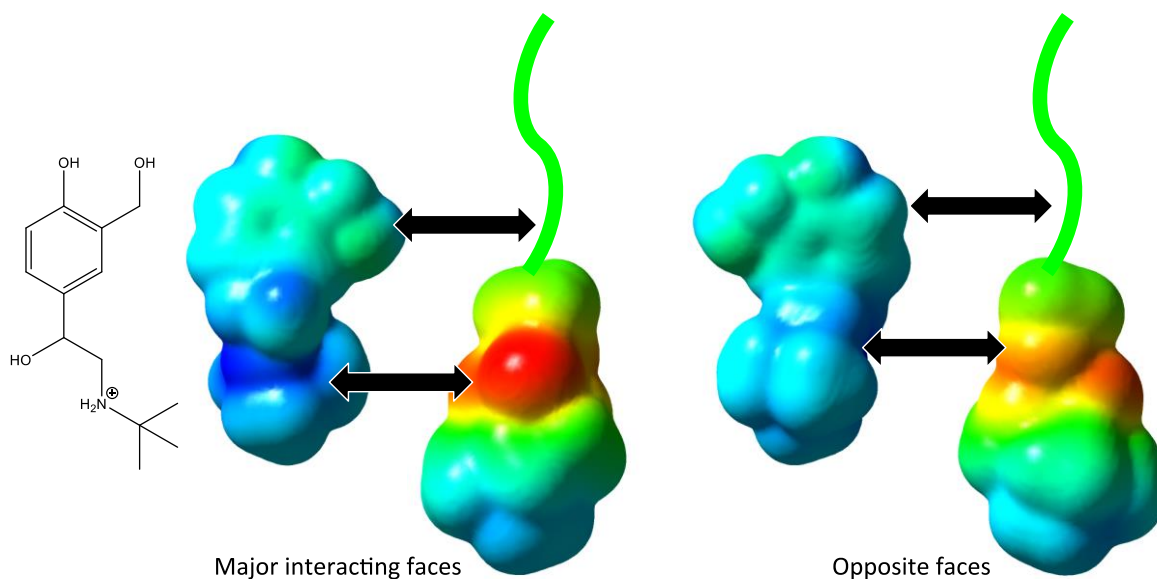
510

511 The electrostatic potential surfaces (EPSs) of the polar head groups associated with each surfactant
512 molecule (i.e. DPPC, POPG and PA) along with salbutamol were calculated via the quantum mechanics
513 software package Gaussian09. The hydrophobic tails were abbreviated to a methyl group, to avoid
514 studying conformations that would not be relevant to the monolayer conditions. A set of up to 10
515 conformations of each molecule was created by omega and each was optimized with RHF/6-31G*.
516 The lowest energy conformation was then identified and its electrostatic potential projected onto a
517 surface of the molecule (the total electron density cut at 0.0004 electrons/Å³). In these electrostatic
518 potential maps, red indicates strongly negative regions, yellow less negative regions, blue strongly
519 positive regions and cyan less positive regions. Regions coloured green have an approximately neutral
520 electrostatic potential. To aid analysis we provide arrows to highlight important regions of interaction
521 and place the linkage to the hydrophobic tails at the top of each figure.

522 In the case of salbutamol, one end of the molecule is generally hydrophobic (the aromatic ring) and
523 this is assumed to prefer contact with the hydrophobic tails of the monolayer and so is also placed at
524 the top of the figure. The EPSs for salbutamol are shown for the molecule in its predominant cationic
525 form. Similar images for the zwitterionic form, in which the phenol is deprotonated, were also
526 generated but represent only a small contribution (i.e. <1%) to the population of molecules and so are
527 not shown here.

528

529



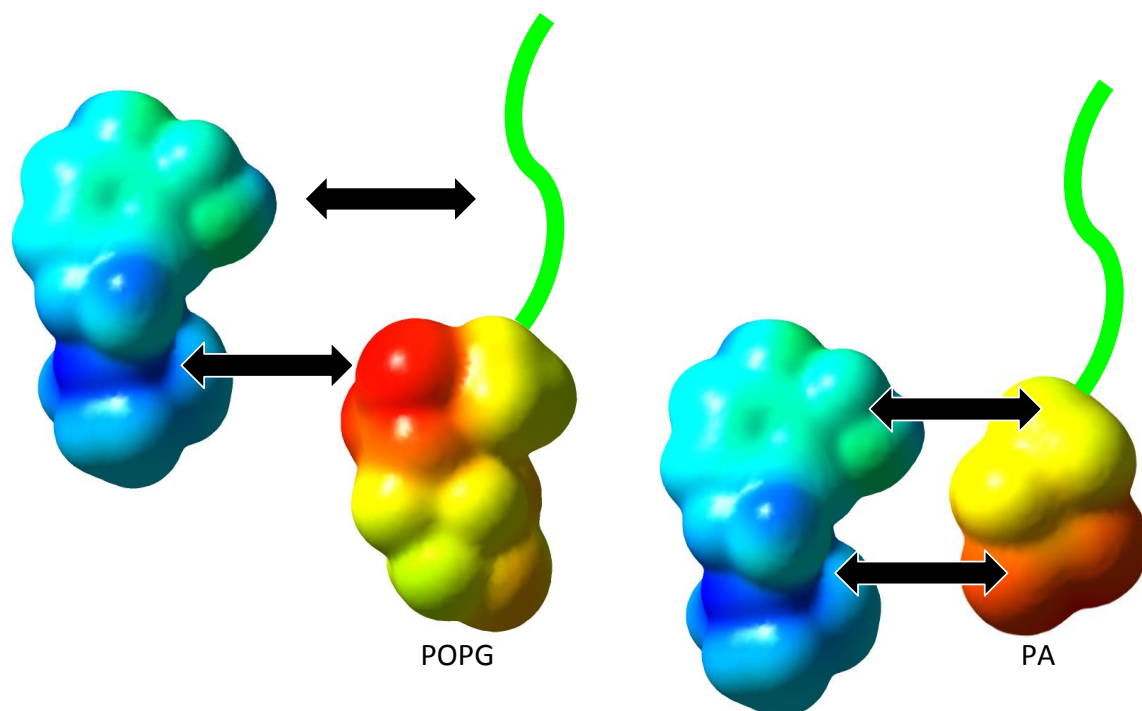
530

531 **Figure 5.** EPS calculations of salbutamol and DPPC (front and rear views provided) with key interaction sites
532 determined for pH 7.

533 When in proximity to DPPC, the predominant component of the monolayer, the two are likely to
534 interact in a way that maximises both electrostatic and hydrophobic interactions. As shown in Figure
535 5, when the major interacting face of salbutamol presents a large positively charged patch in such a
536 way that it can interact with the negatively charged patch to the major interacting face of DPPC, this
537 naturally places the hydrophobic aromatic ring in proximity with the hydrophobic tails of DPPC. When
538 the molecules are paired like this, it can be seen that the opposite face of each molecule are also
539 complementary, albeit with less extreme electrostatic components. When the interactions with the
540 other components of the monolayer are considered, as shown in Figure 6, it is clear that there are a
541 range of positions that salbutamol can adopt to allow it to maximise beneficial interactions with the
542 molecules around it, regardless of which molecules those are. The optimum position in each case
543 involves a different degree of penetration into the monolayer.

544 With POPG, the interactions are likely to be best when the salbutamol penetrates deeply into the
545 monolayer whereas with PA, the opposite is the case. This differing behaviour will cause different
546 effects on the monolayer. When amongst the head groups (as with PA), the salbutamol is promoting
547 the movement apart of the hydrophobic tails and making the monolayer more like the gas phase.
548 Whereas, when the salbutamol penetrates amongst the tail groups (as with POPG and DPPC), it
549 compresses those groups making the system more like the solid phase.

550



551

552 **Figure 6.** *EPS calculations of salbutamol, POPG and PA with key interaction sites determined for pH 7.*

553 These hydrophobic and electrostatic forces of attraction explain the consistent shift of the Langmuir
 554 isotherm and isocycle data as compared to the baseline, which relates to expansion of the monolayer.
 555 The spontaneous movement of drug molecules into the monolayer and the formation of molecular
 556 interactions between the molecules encourage and facilitate drug partitioning and insertion. Thus, the
 557 monolayer is less compressible and highly rigid resulting in an expanded character.

558 **4. Conclusion**

559

560

561 This study has considered the partitioning behaviour of salbutamol (sulphate) when in close proximity
 562 to fundamental components of endogenous pulmonary surfactant. The work confirms the suitability
 563 of Langmuir monolayers to serve as model interfaces to further current understanding within this
 564 relatively under-researched field. The data indicate that the drug molecule of interest impacted upon
 565 the activity of simulated pulmonary surfactant during compression and expansion phases; reflective
 566 of the human breathing cycle. The injection of salbutamol sulphate to the underside of the lipid film
 567 (i.e. to reflect drug availability post particle dissolution) caused general expansion of the surface active
 568 material and decreased the compressibility term. Drug partitioning behaviour was highly dependent
 569 on the physical state of the surfactant monolayer, where the rate of partitioning was greater at the
 570 lower surface pressure that represented greater molecular disorder.

571 Naturally, potential exists to exploit the drug partitioning process in lung surfactant films for
572 therapeutic advantage. The sustained presence of a drug molecule(s) in the pulmonary space could
573 be of clear benefit of the patient in reducing the frequency of daily dosing. Indeed, this approach may
574 be viewed as an advanced modified release strategy (i.e. non-classical) that is solely dependent on
575 chemical complementarity between all species involved.

576

577 5. Acknowledgements

578 MJD would like to thank LJMU for supporting this research effort. Special thanks go to Dr Phil Rowe
579 and Mr Geoffrey Henshaw for the support provided throughout.

580

581 6. References

582

- 583 1. Patton, K.Y., Thibodeau G.A. Structure and Function of the Pulmonary System. Anatomy &
584 Physiology, Ed 8, St Louis, **2013**.
- 585 2. Davies, M.J., Brindley, A., Chen, X., Doughty, S.W., Marlow, M., Shrubbs, I. & Roberts, C.J.
586 Characterization of Drug Particle Surface Energetics and Young's Modulus by Atomic Force
587 Microscopy and Inverse Gas Chromatography. *Pharmaceutical Research*. **2005**, 22(7): 1158 -
588 1166.
- 589 3. Tena, F., Clara P.C. Deposition of Inhaled Particles in the Lungs. *Archivos de Bronconeumología*
590 *(English Edition)*. **2012**, 48(7): 240–246.
- 591 4. Chrystyn, H. Methods to identify drug deposition in the lungs following inhalation. *British*
592 *Journal of Clinical Pharmacology*. **2002**, 51(4): 289-299.
- 593 5. Labiris, N., Dolovich, M. Pulmonary drug delivery. Part I: Physiological factors affecting
594 therapeutic effectiveness of aerosolized medications. *British Journal of Clinical Pharmacology*.
595 **2003**, 56(6): 588-599.
- 596 6. Griese, M. Pulmonary surfactant in health and human lung diseases: State of the art.
597 *European Respiratory Journal*. **1999**, 13(6): 1455-1476.
- 598 7. Hohlfeld, J. The role of surfactant in asthma. *Respiratory Research*. **2002**, 3(1): 4.
- 599 8. Zasadzinski, J.A., Ding J., Warriner H.E., Waring A.J., Bringezu F. The physics and physiology of
600 lung surfactants. *Current Opinion in Colloids and Interface Science*. **2001**, 6(5-6): 506–513.

- 601 9. Bringezu, F., Pinkerton, K.E., Zasadzinski, J. Environmental tobacco smoke effects on the
602 primary lipids of lung surfactant. *Langmuir*. **2003**, 19: 2900-2907.
- 603 10. Davies, M.J., Leach, A.G., Fullwood, D.L., Mistry, D., Hope, A. The pH dependent interaction
604 between nicotine and simulated pulmonary surfactant monolayers with associated molecular
605 modelling. *Surface and Interface Analysis*. **2017**, DOI: 10.1002/sia.6244.
- 606 11. Drugbank.ca. Salbutamol. Available at: www.drugbank.ca/drugs/DB01001. Accessed January
607 2017.
- 608 12. Pinheiro, M., Lucio, M., Reis, S., Giner-Casares, L., Lima, J.L.F.C, Caio J.M, Moiteiro, C., Martin-
609 Romero M.T., Camacho, L. Molecular interaction of rifabutin on model lung surfactant
610 monolayers. *Journal of Physical Chemistry B*. **2012**, 116(38): 11635–11645.
- 611 13. Veldhuizen, R., Haagsman, P.H. The role of lipids in pulmonary surfactant. *Biochimica et*
612 *Biophysica Acta (BBA) - Molecular Basis of Disease*. **1998**, 1408(s 2–3): 90–108.
- 613 14. Goerke, J. Pulmonary surfactant: Functions and molecular composition. *Biochim Biophys Acta*.
614 **1998**, 1408: 79-89.
- 615 15. Moynihan, H, Crean, A. The physicochemical basis of pharmaceuticals, 1st Ed. **2009**. Oxford:
616 Oxford University Press, UK.
- 617 16. Aulton, M.E., Taylor, K.M.G. Aulton's Pharmaceuticals: The Design and Manufacture of
618 Medicines, 4th Ed. **2013**. Churchill Livingstone, China.
- 619 17. Krill, S., Lau, K., Plachy, W., Rehfeld, S. Penetration of dimyristoylphosphatidylcholine
620 monolayers and bilayers by model β -blocker agents of varying lipophilicity. *J Pharm Sci*. **1998**,
621 87(6): 751-756.
- 622 18. BNF 72: British National Formulary 72, 2016. British Medical Association & Royal
623 Pharmaceutical Society of Great Britain.
- 624 19. Lemke, T.L., Williams, D.A., Roche, V.F., Zito, S.W. Foye's principles of medicinal chemistry.
625 Philadelphia, PA: Lippincott Williams & Wilkins. **2013**. 1314–1320.
- 626 20. Chemistry Review Data Sheets - Center for Drug Evaluation and Research (FDA). Available at:
627 www.accessdata.fda.gov/drugsatfda_docs/nda/2011/021747Orig1s000ChemR.pdf.
628 Accessed January 2017.
- 629 21. Clark, T., Hennemann, M., Murray, J.S., Politzer, P. Halogen bonding: the σ -hole. *Journal of*
630 *Molecular Modelling*. **2007**, 13: 291-296.
- 631 22. Hunter, A.C. Quantifying Intermolecular Interactions: Guidelines for the molecular recognition
632 toolbox. *Angew. Chem. Int. Ed.* **43**. **2004**, 5310-5324.
- 633 23. Sherwood, L., Human Physiology: From Cells to Systems. 7th Ed. **2010**. Brooks / Cole Cengage
634 Learning, United States of America.

- 635 24. Shah A.R, Banerjee R. Effect of D- α -tocopheryl polyethylene glycol 1000 succinate (TPGS) on
636 surfactant monolayers. *Colloids Surf B*. **2011**, 85: 116-124.
- 637 25. Subramaniam, S., Bummer, P., Gairola, C.G. Biochemical and Biophysical Characterization of
638 Pulmonary Surfactant in Rats Exposed Chronically to Cigarette Smoke. *Fundamental and*
639 *Applied Toxicology*. **1995**, 27:63-69.
- 640 26. Minitab v17. Available at: www.minitab.com. Accessed January 2017.
- 641 27. Roothaan, C.C.J. New developments in molecular orbital theory. *Reviews of Modern Physics*.
642 **1951**, 23: 69.
- 643 28. Hall, G.G. In the molecular orbital theory of chemical valency. VIII. A method of calculating
644 ionization potentials. Proceedings of the Royal Society of London A: Mathematical, Physical
645 and Engineering Sciences; *The Royal Society*. **1951**, 205: 541-552.
- 646 29. Hariharan, P.C., Pople, J.A. Influence of polarization functions on MO hydrogenation energies.
647 *Theor. Chim. Acta*. **1973**, 28: 213-222.
- 648 30. Gaussian 09, Revision C.01. M.J. Frisch, G.W. Trucks, H.B. Schlegel, G.E. Scuseria, M.A. Robb,
649 J.R. Cheeseman, G. Scalmani, V. Barone, B. Mennucci, G.A. Petersson, H. Nakatsuji, M.
650 Caricato, X. Li, H.P. Hratchian, A.F. Izmaylov, J. Bloino, G. Zheng, J.L. Sonnenberg, M. Hada, M.
651 Ehara, K. Toyota, R. Fukuda, J. Hasegawa, M. Ishida, T. Nakajima, Y. Honda, O. Kitao, H. Nakai,
652 T. Vreven, J.A. Montgomery, J.E. Peralta, F. Ogliaro, M. Bearpark, J.J. Heyd, E. Brothers, K.N.
653 Kudin, V.N. Staroverov, R. Kobayashi, J. Normand, K. Raghavachari, A. Rendell, J.C. Burant, S.S.
654 Iyengar, J. Tomasi, M. Cossi, N. Rega, J.M. Millam, M. Klene, J.E. Knox, J.B. Cross, V. Bakken, C.
655 Adamo, J. Jaramillo, R. Gomperts, R.E. Stratmann, O. Yazyev, A.J. Austin, R. Cammi, C. Pomelli,
656 J.W. Ochterski, R.L. Martin, K. Morokuma, V.G. Zakrzewski, G.A. Voth, P. Salvador, J.J.
657 Dannenberg, S. Dapprich, A.D. Daniels, Ö. Farkas, J.B. Foresman, J.V. Ortiz, J. Cioslowski, D.J.
658 Fox. Gaussian, Inc., Wallingford CT, 2009.
- 659 31. Omega, Version 2.5.1.4, OpenEye Scientific Software, Inc., Santa Fe, NM, USA,
660 www.eyesopen.com, 2010.
- 661 32. GaussView, Version 5, Dennington, Roy; Keith, Todd; Millam, John. Semichem Inc., Shawnee
662 Mission, KS, 2009.
- 663 33. Matti, V., Saily, J., Ryhanen, S.J., Holopainen, J.M., Borocci, S., Mancini, G., Kinnunen, P.K.
664 Characterization of mixed monolayers of phosphatidylcholine and a dicationic gemini
665 surfactant SS-1 with a Langmuir balance: Effects of DNA. *Biophys J*. **2001**, 81(4): 2135-2143.
- 666 34. Boggara, M., Krishnamoorti, R. Partitioning of nonsteroidal antiinflammatory drugs in lipid
667 membranes: A molecular dynamics simulation study' *Biop J*. **2010**, 98(4): 586-595.

- 668 35. Jabłonowska, E., Bilewicz, R. Interactions of ibuprofen with Langmuir monolayers of
669 membrane lipids *Thin Solid Films*. **2007**, 515(7-8): 3962-3966.
- 670 36. Davies, M.J., Kerry, T.D., Seton, L., Murphy, M.F., Gibbons, P. Khoo, J. & Naderi, M. The crystal
671 engineering of salbutamol sulphate via simulated pulmonary surfactant monolayers.
672 *International Journal of Pharmaceutics*. **2013**, 446: 34-45.
- 673 37. Faller, R., Jue, T., Longo, L.M., Risbud, H.S. Biomembrane Frontiers - Nanoparticles, Models
674 and the Design of Life, Structure and dynamics of lipid monolayers: theory and applications.
675 Chapter 4 (2). **2012**, Humana Press, Online.
- 676 38. Curosurf. Available at www.curosurf.com. Accessed January 2017.
- 677 39. Vilallonga, F.A., Phillips, E.W. Interaction of doxorubicin with phospholipid monolayers.
678 *Journal of Pharmaceutical Sciences*. **1978**, 67(6): 773 – 775.
- 679 40. Davies, M.J., Seton, L., Tiernan, N., Murphy, M.F., Gibbons, P. Towards crystal engineering via
680 simulated pulmonary surfactant monolayers to optimise inhaled drug delivery. *International*
681 *Journal of Pharmaceutics*. **2011**, 421: 1–11.
- 682 41. Minones, J., Patino, J.M.R., Conde, O., Carrera, C., Seoane, R. The effect of polar groups on
683 structural characteristics of phospholipid monolayers spread at the air–water interface.
684 *Colloids Surf. A: Physicochem. Eng. Aspects*. **2002**, 203: 273–286.
- 685 42. McGregor, M.A., Barnes, G.T. The equilibrium penetration of monolayers. *Journal of Colloid*
686 *and Interface Science*. **1978**, 65(2): 291 – 295.
- 687 43. McGregor, M.A., Barnes, G.T. Equilibrium penetration of monolayers VI: Cholesterol-
688 cetrimonium bromide system. *Journal of Pharmaceutical Sciences*. **1978**, 67(8): 1054 – 1056.
- 689 44. Davies, M.J., Birkett, J.W., Kotwa, M., Tomlinson, L., Woldetinsae, R. The impact of cigarette/e-
690 cigarette vapour on simulated pulmonary surfactant monolayers under physiologically
691 relevant conditions. *Surface and Interface Analysis*. **2017**, DOI: 10.1002/sia.6205.
- 692
- 693
- 694
- 695
- 696
- 697
- 698